Available online at www.sciencedirect.com
ScienceDirect
Trans. Nonferrous Met. Soc. China 23(2013) 3412−3420
Transactions of Nonferrous Metals Society of China
www.tnmsc.cn

# Ultra fine grinding of silver plant tailings of refractory ore using vertical stirred media mill

O. CELEP, E. Y. YAZICI

UFG Group, Division of Mineral & Coal Processing, Department of Mining Engineering, Karadeniz Technical University, Trabzon 61080, Turkiye

Received 21 March 2013; accepted 25 April 2013

**Abstract:** Ultra fine grinding of the plant tailings of a refractory silver ore was studied using a laboratory type vertical stirred media mill. Preliminary tests confirmed that ultra fine grinding substantially improves the extraction of silver from the tailings in cyanide leaching (i.e. 36% Ag extraction rate from the as-received tailings with $d_{80}$ of 100 μm, c.f. 84% extraction rate after ultra fine grinding of the tailings with $d_{80}$ of 1.2 μm). In the ultra fine grinding tests, the effects of ball diameter (2−4.5 mm), stirring speed (200−800 r/min) and ball charge ratio (50%−80%) on the fineness of grind ($d_{80}$, μm) were investigated through a Box–Behnken design. Increasing stirrer speed and ball charge ratio decreased fineness of grind while larger balls resulted in the coarser products. The tests demonstrated that a fineness of grind less than 5 μm can be achieved under suitable conditions. Analysis of stress intensity indicated an optimum range of stress intensity of $(0.8-2)\times10^{-3}$ N·m for all power inputs.

**Key words:** refractory ore tailings; stirred media mill; ultra fine grinding; experimental design; Box–Behnken design; stress intensity

## 1 Introduction

Refractory ores yield low extractions rates (i.e. <80%) of gold and silver in cyanide leaching even after grinding the ore down to −75 μm. These ores need a suitable pretreatment to achieve high gold and silver extractions rates during cyanidation [1]. Roasting [2], pressure oxidation [3], biooxidation [4,5] and ultra fine grinding [6] have been commercially practiced to enhance the gold/silver recoveries from refractory ores. The most common cause of refractoriness in gold and silver ores is the encapsulation of fine gold and silver particles within the mineral matrix in which these particles are not accessible to the lixiviating action of cyanide and oxygen [7]. If the encapsulated gold is 1−2 μm to approximately 20 μm in size, a desired degree of liberation can be suitably achieved by ultra fine grinding (UFG) without the need for costly and environmentally unfavorable chemical pretreatments [6,8].

In the last 20 years, the stirred media mills have been widely used for ultra fine grinding in different industrial fields such as mineral processing, plastic, ceramics, paint, food and cosmetic [9,10]. Vertimill®, Stirred Media Detritor (SMD®) and ISAMill® have been the most commonly used stirred media mills in mineral processing. The various types (e.g. glass, steel, ceramic, pebble etc.) and sizes (usually between 200 and 4000 μm) of grinding media were used depending on the feed size and feed material [11,12].

Various process parameters including stirrer speed, ball diameter, ball charge ratio and media density as well as mineral type affect the performance of a grinding process [11,13−18]. Many studies have been carried out to examine the operating parameters affecting the grinding performance of stirred media mills [15,16,19]. One classical factor at a time approach may fail in determining main and interaction effects together and optimising grinding parameters [20]. In this respect, the statistical experimental design methods can be suitably utilized to assess the main/interaction effects of parameters. Response surface methodology (RSM) is widely used since it combines mathematical and statistical methods [8,21−24]. Stress intensity analysis of grinding media based on grinding parameters such as stirrer speed, ball diameter and media height as well as slurry density, can be used to identify the optimum conditions at a given energy consumption [9,11].

**Corresponding author:** O. CELEP; Tel: +90-462-377-4118; Fax: +90-462-325-7405; E-mail: ocelep@ktu.edu.tr
DOI: 10.1016/S1003-6326(13)62882-4

Recently, application of ultra fine grinding using stirred media mills for the treatment of refractory gold and platinum ores prior to leaching, has been increased dramatically to improve the metal recoveries [25,26]. Old plant tailings, which were produced by conventional comminution circuits, may also contain substantial amount of precious metals. Chemical pretreatment of such tailings may fail to improve the extraction of precious metals [27]. Ultra fine grinding as a pretreatment step can be exploited as a potentially new approach for reprocessing of such plant tailings to recover contained metal/mineral values, which would also contribute to the conservation of natural resources.

In this study, the ultra fine grinding of the plant tailings of a refractory silver ore was studied to recover the contained silver in subsequent cyanidation. The effects of ball diameter (2−4.5 mm), stirring speed (200−800 r/min) and ball charge ratio (50%−80%) on the ultra fine grinding process were investigated using a laboratory type vertical stirred media mill. Response surface methodology, a three-level Box–Behnken design, was adopted to assess the effect of parameters on the response, i.e. particle size ($d_{80}$) of the product. Grinding efficiency in terms of stress number and intensity concept was also evaluated.

## 2 Materials and methods

### 2.1 Tailing sample and preliminary cyanidation tests

The plant tailings after cyanide leaching ($d_{80}$=100 μm) of a refractory silver ore were used in this work. The chemical composition of the ore sample was determined by wet chemical analysis method using ICP–AES (inductively coupled plasma–atomic emission spectroscopy), NAA (neutron activation analysis) after hot digestion in aqua regia for Au–Ag analysis and XRF analysis for major oxides. The tailing sample consisted of 50.7% $SiO_2$, 9.80% BaO, 7.30% $Al_2O_3$, 6.76% CaO and 5.72% $Fe_2O_3$. The sample was determined to be rich in silver containing 83 g/t Ag and 1.5 g/t Au. Earlier mineralogical studies on the tailings have shown that silver is present mainly in the form of native silver, pyrargyrite, tetrahedrite, argentite and proustite, which are closely associated with and/or encapsulated in other mineral phases, i.e. mainly barite, quartz, dolomite and feldspar [27]. Earlier studies have confirmed poor extraction of silver even after various chemical pretreatments of the tailings [27]. Details of the procedure for cyanide leaching and chemical analysis can be found elsewhere [28].

### 2.2 Ultra fine grinding tests

Ultra fine grinding experiments were performed using a laboratory scale pin-type vertical stirred media mill designed by the authors (Fig. 1) within a batch mode of operation. The technical features of the stirred media mill were described earlier by CELEP et al [8]. Energy consumptions in the grinding tests were measured using an electrical counter connected to the stirrer rotor. Micro-grinding ceramic beads (alumina-based zirconia toughened, DMM AZ 2000®) with different sizes (mean diameters of 2, 3.5 and 4.5 mm) were kindly provided by Dakot Milling Media (Pty) Ltd. (South Africa) and used as the grinding media. The beads had $Al_2O_3$ content of 80%, specific gravity (SG) of 3.75–3.80 and Vickers hardness (HV) of 1314 μm. Utilization of inert ceramic grinding media would avoid/limit adverse effects of steel media during leaching through formation and subsequent coating of iron oxide on mineral surfaces [29]. In the tests, the pulp density was kept at 24% (w/v). Analysis of particle size of the samples was carried out by the laser diffraction method using a Malvern Mastersizer 2000 MU. Particle size analysis was performed in four replicates (RSD: 0.71%) and the mean values were present in the results.

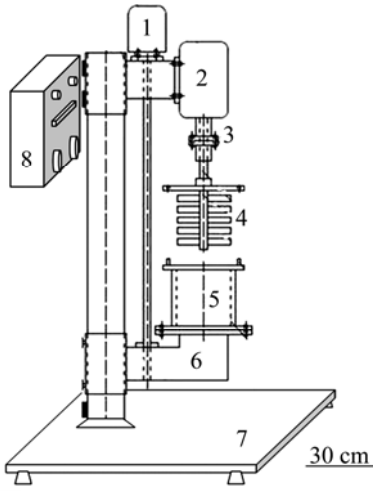


**Fig. 1** Section drawing of stirred mill used in ultrafine grinding tests [8] (1—Motor for moving of grinding chamber; 2—Motor of stirring shaft; 3—Connection of motor and shaft; 4—Stirring pins; 5—Grinding chamber; 6—Moving table of stirred grinding chamber; 7—Stability table; 8—Control panel)

### 2.3 Experimental design

Response surface methodology (RSM) involves the utilization of mathematical and statistical techniques and allows the evaluation of contribution of several independent parameters (variables) on the response. A Box–Behnken design (BBD), essentially a type of RSM, has three levels, low (−1), center (0) and high (+1) as coded levels, with equally spaced intervals among these levels. Actual levels can be calculated by [30]

$$X_{\text{center}} = \frac{X_{\text{high}} - X_{\text{low}}}{2} \quad (1)$$

The relationship between the coded and actual (uncoded) values can be obtained by

$$x_{\text{coded}} = \frac{X_{\text{actual}} - X_{\text{center}}}{X_{\text{center}} - X_{\text{min}}} \quad (2)$$

where $x_{\text{coded}}$ is coded value; $X_{\text{actual}}$, $X_{\text{center}}$ and $X_{\text{min}}$ are corresponding actual value, actual value in the center and minimum (low) actual value, respectively. The number of experiments ($N$) required for a Box–Behnken design can be calculated as

$$N=n^2+n+c_{\text{p}} \quad (3)$$

where $n$ and $c_{\text{p}}$ are the number of parameters and replicates in the central point, respectively [21,30]. Accordingly, 15 experiments are needed for a three-variable design ($n$=3) with three replicate experiments ($c_{\text{p}}$=3) in the central point. A second-order mathematical model can be built to estimate the response ($Y$) based on the experimental data.

$$Y = \beta_0 + \beta_1 x_1 + \beta_2 x_2 + \beta_3 x_3 + \beta_{11} x_1^2 + \beta_{22} x_2^2 + \beta_{33} x_3^2 + \beta_{12} x_1 x_2 + \beta_{13} x_1 x_3 + \beta_{23} x_2 x_3 \quad (4)$$

where $Y$ is the predicted response; $\beta_0$ is the model constant; $x_1$, $x_2$, $x_3$ and $x_4$ are independent variables; $\beta_1$, $\beta_2$, $\beta_3$ and $\beta_4$ are linear coefficients; $\beta_{12}$, $\beta_{13}$ and $\beta_{23}$ are interaction coefficients; $\beta_{11}$, $\beta_{22}$ and $\beta_{33}$ are the quadratic coefficients [20,30].

In the current study, BBD was adopted to assess the effect of the parameters (i.e. ball diameter, stirrer speed and ball charge ratio) on the particle size ($d_{80}$) of the ground material over 15 min of grinding. Selected variables and their corresponding levels in the ultra fine grinding tests are presented in Table 1. Minitab [31] and Design−Expert [32] software were used to perform the statistical analysis of the experimental data.

**Table 1** Parameters and their corresponding coded and actual levels

| Parameter | Symbol | | Coded level | | |
|---|---|---|---|---|---|
| | Actual | Coded | Low (−1) | Center (0) | High (+1) |
| Ball diameter/mm [a] | $X_1$ | $x_1$ | 2 | 3.5 | 4.5 |
| Stirring speed/(r·min$^{-1}$) | $X_2$ | $x_2$ | 200 [b] | 500 [c] | 800 [d] |
| Ball charge ratio/% | $X_3$ | $x_3$ | 50 | 65 | 80 |

[a] Due to practical reasons, selected ball diameters do not match precisely with BBD's experimental layout; [b] 0.77 m/s; [c] 1.92 m/s; [d] 3.07 m/s.

### 2.4 Stress number and intensity of grinding media

In stirred media mills, comminution process is controlled intimately by the number ($N_{\text{s}}$) and intensity ($I_{\text{s}}$) of the stress generated within the grinding environment. Stress number is referred as the average number of stress events of each product particle and affects product fineness for a given stress intensity and expressed as [14,33]

$$N_{\text{s}} = \frac{N_{\text{c}} P_{\text{s}}}{N_{\text{p}}} \quad (5)$$

where $N_{\text{c}}$, $P_{\text{s}}$ and $N_{\text{p}}$ are the number of media contacts, the probability of stressing of a particle at a media contact and the number of product particles inside the mill, respectively. In the case of grinding of crystalline materials, the following proportionality is derived [14].

$$N_{\text{s}} \propto \frac{\varphi_{\text{GM}}(1-\varepsilon)}{[1-\varphi_{\text{GM}}(1-\varepsilon)]c_{\text{v}}} \frac{nt}{d_{\text{GM}}^2} \quad (6)$$

where $n$ is the number of revolutions of the stirrer per unit time, $t$ is the grinding time, $\varphi_{\text{GM}}$ is the filling ratio of the grinding media, $\varepsilon$ is the porosity of the bulk of grinding media, $d_{\text{GM}}$ is the diameter of the grinding media, and $c_{\text{v}}$ is the volume concentration of the pulp.

Stress intensity describes the energy involved in a breakage event. There is an optimal range for this energy required to break a particle. When the stress intensity produced is smaller than the required level, the number of stress events should be increased to break a particle, i.e. low breakage rate. The stress intensity beyond the optimum range will lead to the excessive consumption of energy [11]. Stress intensity analysis was primarily developed for high-speed horizontal stirred media mills in which grinding event is governed mainly by centrifugal forces. In low-speed vertical stirred media mills, gravity forces also take action [11,34]. Centrifugal forces become more important at high stirring speeds (i.e. a tip speed of >3 m/s) in a pin type vertical mill while the gravitational forces are more dominant at low stirring speeds (<3 m/s), particularly for industrial applications where media height is up to 2 m [34]. The gravitational ($I_{\text{gm}}$) and centrifugal stress intensities ($I_{\text{sm}}$ where the modulus of elasticity of the feed material is smaller than that of grinding media) can be expressed by Eq. (7) and Eq. (8), respectively [11,35].

$$I_{\text{gm}} \propto D_{\text{m}}^2(\rho_{\text{m}} - \rho)gh \quad (7)$$

$$I_{\text{sm}} \propto D_{\text{m}}^3(\rho_{\text{m}} - \rho)v_{\text{t}}^2 \quad (8)$$

where $I_{\text{gm}}$ and $I_{\text{sm}}$ are gravitational and centrifugal stress intensities of the grinding media, respectively; $D_{\text{m}}$ is the grinding media size; $\rho_{\text{m}}$ is the grinding media density; $\rho$ is the slurry density; $g$ is the gravitational constant; $h$ is the media height; $v_{\text{t}}$ is the stirrer tip speed.

It can be seen from Eqs. (7) and (8) that in a vertical stirred media mill, stress intensity reflects the combined effects of stirring speed (or media height), media size and density as well as slurry density [34,35]. In this respect,

the performance of a stirred mill as a function of those grinding parameters can be evaluated by analysis of stress intensity [35]. In this study, the stress number and intensity were calculated using the data obtained and plotted as a function of product particle size ($d_{80}$).

## 3 Results and discussion

### 3.1 Preliminary cyanidation tests

Ultra fine grinding of the tailings can substantially enhance the cyanide leaching of silver, i.e. 84% silver extraction rate after ultra fine grinding ($d_{80}$=1.2 μm) even at 1 h, while only 36% extraction rate for the as-received tailings ($d_{80}$=100 μm) (Fig. 2). This suggests that ultra fine grinding is a suitable pretreatment method for the tailings. Therefore, ultra fine grinding of the tailings was studied and the effects of grinding parameters were evaluated using Box−Behnken design as well as stress intensity/number approach.

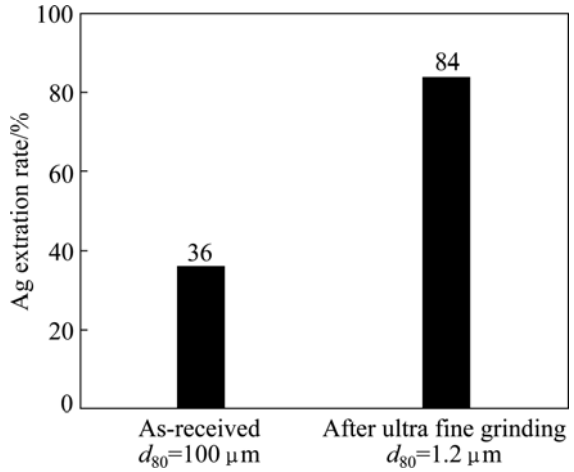


**Fig. 2** Effect of particle size on extraction of silver in cyanide solutions (1.5 g/L NaCN; pH 10.5; temperature: (25±3) °C; flow rate of air: 0.3 L/min; pulp density: 24% (w/v))

### 3.2 Effect of grinding time

Fineness of grind (expressed as $d_{80}$) obtained for different grinding periods (i.e. 1, 4 and 15 min) was used to assess the effect of grinding time under the different conditions of stirring speeds, ball diameters and ball charge ratios (Fig. 3). The increase in grinding time from 1 to 15 min had an important effect on the fineness of the product (Fig. 3). Longer periods (>4 min) were needed to achieve $d_{80}$<5 μm. Accordingly, a constant grinding time of 15 min was taken for the design of grinding tests. Figure 3 also reflects the effect of stirring speed, ball diameter and ball charge ratio on $d_{80}$ of the product as a function of grinding time. It can be concluded that increasing stirring speed and ball charge ratio or using small balls leads to the finer products. Furthermore,

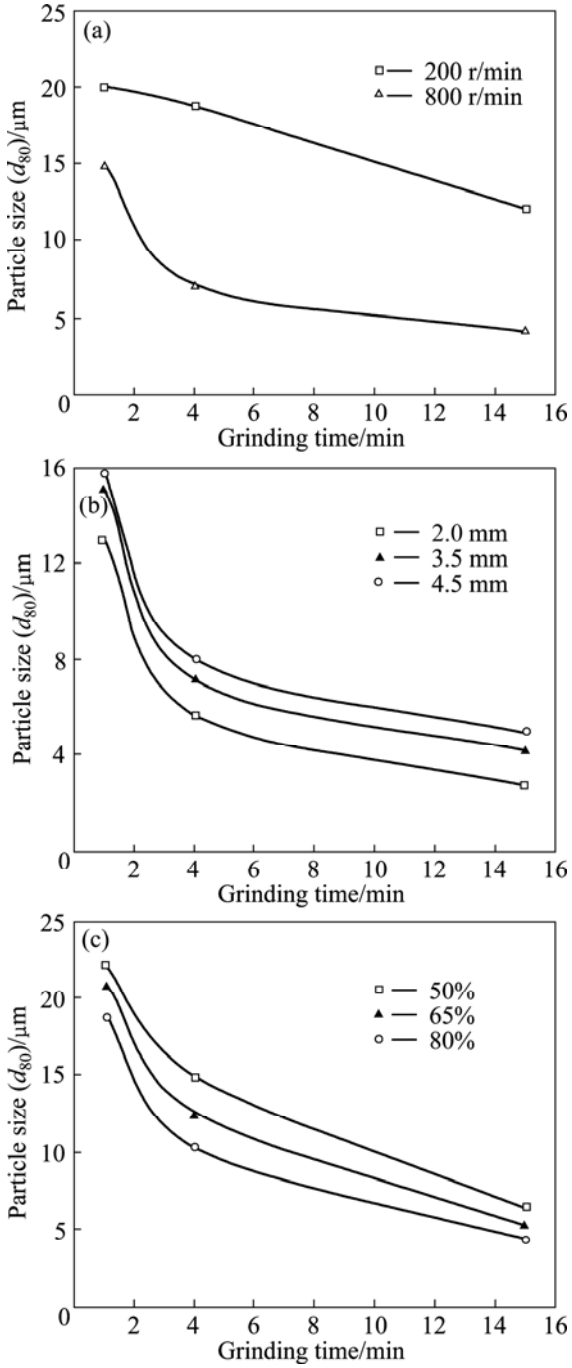


**Fig. 3** Effect of grinding time on particle size ($d_{80}$) with different parameters: (a) Stirring speed (3.5 mm ball diameter, 80% ball charge ratio); (b) Ball diameter (800 r/min stirring speed, 80% ball charge ratio); (c) Ball charge ratio (2 mm ball diameter, 500 r/min stirring speed)

the relative contribution of these parameters to the fineness of product was further evaluated by the Box−Behnken design below.

### 3.3 Evaluation of experimental data

The experimental layout produced by Box−Behnken design for 15 experiments is shown in Table 2. Parameter combinations with coded/actual values for each

experiment and observed/predicted results ($d_{80}$) are also included in Table 2. The predicted values were estimated by the regression model described in Section 3.3.1. The relative standard deviation (RSD) of the data was calculated as 2.31%.

3.3.1 Modelling and statistical analysis

The observed experimental results ($d_{80}$) (Table 2) were employed to establish a second-order regression model. An unknown response ($Y$ in $d_{80}$) can be estimated for any coded level of ball diameter ($x_1$), stirrer speed ($x_2$) and ball charge ratio ($x_3$).

$$Y = 6.52 + 1.28x_1 - 4.27x_2 - 1.52x_3 - 1.07x_1^2 + 2.81x_2^2 + 0.88x_3^2 - 0.45x_1x_2 + 0.08x_1x_3 + 1.11x_2x_3 \quad (9)$$

The analysis of variance (ANOVA) for the regression model and linear/square/interaction contributions is presented in Table 3. $P$ values were used for the significance test. The $P$ value shows the probability that the test statistic will take on a value that is at least as extreme as the observed value of the statistic when the null hypothesis ($H_0$) holds true. Simply, a $P$ value <0.05 suggests that the null hypothesis is rejectd). If the $P$ value is lower than the confidence level in the significance test, it is statistically significant according to the selected confidence level. For example, if $P$=0.04 <$\alpha$=0.05, it shows the significance of a parameter at a confidence level of 95% ($\alpha$=0.05) [21]. In this respect, the $P$ value (<0.001) of the regression model confirms the adequacy of the model, i.e. statistically significant even at 99.5% ($\alpha$=0.005) confidence level (Table 3). The linear (main) and square (quadratic) contributions were also found to be significant at 95% ($\alpha$=0.05) and interactions were found to be insignificant.

Table 4 shows the estimated regression coefficients used to construct the model with their statistical significance test. It was also confirmed that all the linear (main) and square (quadratic) effects were significant at

**Table 2** Box-Behnken design layout with coded and actual values with observed results ($d_{80}$)

| Experimental No. | Level of parameter | | | | | | $d_{80}$/μm | |
|---|---|---|---|---|---|---|---|---|
| | Coded | | | Actual | | | Observed | Predicted |
| | $x_1$ | $x_2$ | $x_3$ | $X_1$/mm | $X_2$/(r·min$^{-1}$) | $X_3$/% | | |
| 1 | −1 | −1 | 0 | 2 | 200 | 65 | 9.72 | 10.80 |
| 2 | +1 | −1 | 0 | 4.5 | 200 | 65 | 13.8 | 14.25 |
| 3 | −1 | +1 | 0 | 2 | 800 | 65 | 3.64 | 3.16 |
| 4 | +1 | +1 | 0 | 4.5 | 800 | 65 | 5.90 | 4.82 |
| 5 | −1 | 0 | −1 | 2 | 500 | 50 | 6.34 | 6.64 |
| 6 | +1 | 0 | −1 | 4.5 | 500 | 50 | 8.15 | 9.05 |
| 7 | −1 | 0 | +1 | 2 | 500 | 80 | 4.35 | 3.45 |
| 8 | +1 | 0 | +1 | 4.5 | 500 | 80 | 6.46 | 6.16 |
| 9 | 0 | −1 | −1 | 3.5 | 200 | 50 | 18.5 | 17.11 |
| 10 | 0 | +1 | −1 | 3.5 | 800 | 50 | 6.18 | 6.35 |
| 11 | 0 | −1 | +1 | 3.5 | 200 | 80 | 12.0 | 11.85 |
| 12 | 0 | +1 | +1 | 3.5 | 800 | 80 | 4.15 | 5.53 |
| 13 | 0 | 0 | 0 | 3.5 | 500 | 65 | 6.42 | 6.52 |
| 14 | 0 | 0 | 0 | 3.5 | 500 | 65 | 6.69 | 6.52 |
| 15 | 0 | 0 | 0 | 3.5 | 500 | 65 | 6.45 | 6.52 |

**Table 3** Analysis of variance (ANOVA) for regression model

| Source | Degree of freedom | Sum of square | Adjusted sum of square | Adjusted mean square | $P$ value | Contribution/% |
|---|---|---|---|---|---|---|
| Regression model | 9 | 220.514 | 220.514 | 24.5016 | 0.004 | 96.3 |
| Linear | 3 | 177.309 | 177.309 | 59.1031 | 0.001 | 77.4 |
| Square | 3 | 37.447 | 37.447 | 12.4822 | 0.028 | 16.4 |
| Interaction | 3 | 5.759 | 5.759 | 1.9195 | 0.420 | 2.51 |
| Residual error | 5 | 8.474 | 8.474 | 1.6949 | | 3.70 |
| Total | 14 | 228.989 | | | | 100 |

**Table 4** Estimated regression coefficients and test of statistical significance for analysis of model terms

| Item | Symbol | Regression coefficient | Standard error of coefficient | *P* value |
|---|---|---|---|---|
| Constant | $\beta_0$ | 6.52067 | 0.7516 | 0.000 |
| Ball diameter | $\beta_1$ | 1.27888 | 0.4603 | 0.039 |
| Stirring speed | $\beta_2$ | −4.26800 | 0.4603 | 0.000 |
| Ball charge ratio | $\beta_3$ | −1.52062 | 0.4603 | 0.021 |
| Ball diameter−ball diameter | $\beta_{11}$ | −1.07258 | 0.6775 | 0.174 |
| Stirring speed−stirring speed | $\beta_{22}$ | 2.80967 | 0.6775 | 0.009 |
| Ball charge ratio−ball charge ratio | $\beta_{33}$ | 0.87942 | 0.6775 | 0.251 |
| Ball diameter−stirring speed | $\beta_{12}$ | −0.44875 | 0.6509 | 0.521 |
| Ball diameter−ball charge ratio | $\beta_{13}$ | 0.07500 | 0.6509 | 0.913 |
| Stirrer speed−ball charge ratio | $\beta_{23}$ | 1.11025 | 0.6509 | 0.149 |

95% ($\alpha$=0.05) with the exception of quadratic effect of ball diameter, i.e. $P$>0.05. The contributions show the relative impact of linear, square and interaction effects with the linear effects being the most dominant (77.4%) (Table 3). It can be inferred from the absolute values of the regression coefficients (Table 4) that the order of significance of linear (main) effects was stirring speed>ball charge ratio>ball diameter. The mode and magnitude of effects can be observed from the response surface plots (see Section 3.3.2). The coefficient of multiple determinations ($R^2$) for the regression model was found to be 0.96 (Fig. 4).

Further grinding tests apart from Box−Behnken design were also performed to test/verify the regression model. Parameter combinations for the tests with the observed and the predicted results are presented in Table 5. It can be noted that, in the 16th run the finest particle size ($d_{80}$=2.73 μm) was obtained (Table 5) under the conditions of 2 mm ball diameter, 800 r/min stirring speed and 80% ball charge ratio.

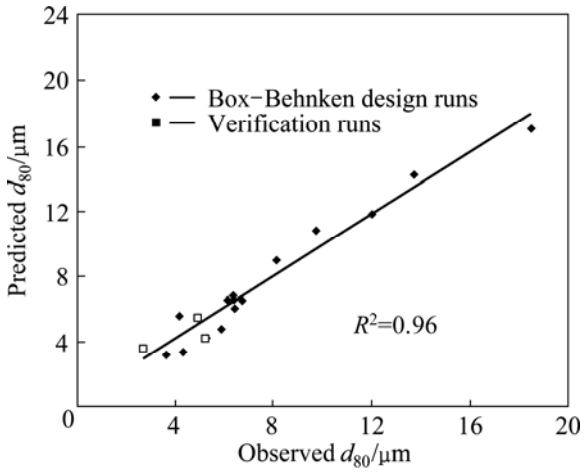


**Fig. 4** Correlation between observed and predicted $d_{80}$

3.3.2 Response surface plots of parameters

Regression equations can be used to derive response surface plots for couples of variables. These plots are practical in terms of simultaneous observation of the effects of dual variables on the response. In the current study, three surface plots were produced by showing the simultaneous effects of two parameters on the particle size ($d_{80}$) while the third parameter was held at the center level (Fig. 5).

Figure 5(a) shows that the increase in stirring speed resulted in a finer product at all levels of ball diameter while larger balls led to a coarser product. As also confirmed by the statistical analysis (Table 4), stirring speed had a greater effect than the ball diameter. Increasing the stirring speed from 200 to 800 r/min (i.e. the 9th and 10th runs, 3.5 mm ball diameter, 50% ball charge ratio) produced one third finer material. CELEP et al [8] also reported that when the stirring speed was increased from 250 to 750 r/min, the product particle size ($d_{80}$) decreased from 9 μm to 4 μm when using 1 mm balls in diameter. In contrast to the findings in the current study (Figs. 5(a) and (c)), previous researchers [10,18, 36] reported that high speeds (up to 1350 r/min) resulted in an increase in the mean particle size with a reduction in the energy efficiency. This adverse effect of stirring speed at high levels can be attributed to the occurrence of central vortex during grinding which increased energy consumption dramatically [14,36].

**Table 5** Verification experiments with observed/predicted $d_{80}$

| Experimental No. | Ball diameter level | Stirring speed level | Ball charge ratio level | $d_{80}$/μm | |
|---|---|---|---|---|---|
| | | | | Observed | Predicted |
| 16 | −1 (2 mm) | +1 (800 r/min) | +1 (80%) | 2.73 | 3.55 |
| 17 | +1 (4.5 mm) | +1 (800 r/min) | +1 (80%) | 4.91 | 5.36 |
| 18 | −1 (2 mm) | 0 (500 r/min) | 0 (65%) | 5.26 | 4.17 |

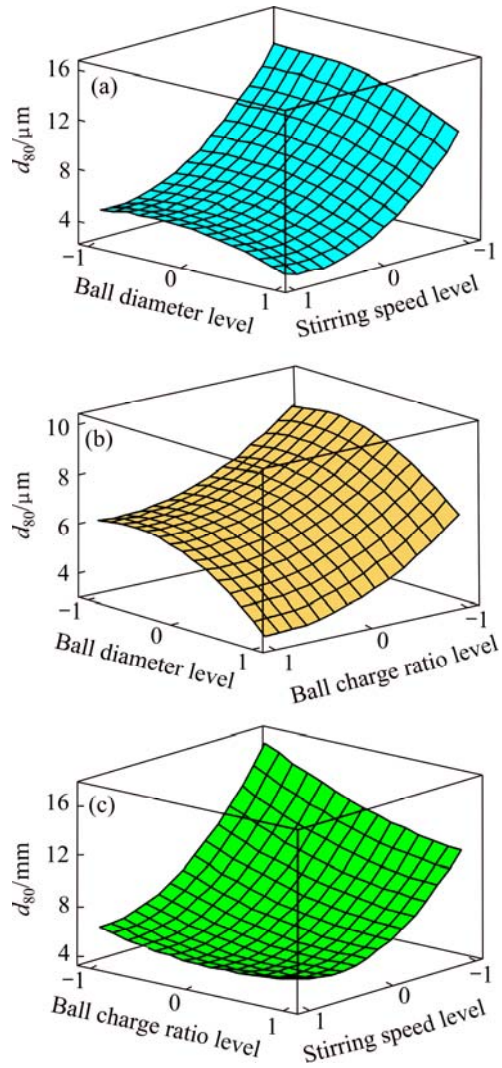


**Fig. 5** Surface plots reflecting simultaneous effect of dual variables on particle size $d_{80}$ (Three variables are held at centre level): (a) Ball diameter and stirring speed; (b) Ball diameter and ball charge ratio; (c) Ball charge ratio and stirring speed

Selection of ball diameter is also of importance regarding stirred milling efficiency and energy consumption [37]. Smaller media are required to obtain finer products, namely, the decrease in ball diameter from 4.5 to 2 mm (the 5th and 6th runs, 500 r/min stirring speed, 50% ball charge ratio) reduced the particle size ($d_{80}$) from 8.15 to 6.34 μm. It was suggested that optimum ball-to-particle size ratio should be selected as 20:1 for the maximum breakage rate [38]. However, the ratio may vary from 7:1 to 20:1 depending on the content/quantity of minerals in the ore and type of grinding media [15]. In the current study, the ball-to-particle size ratio varied between 8:1 and 18:1. Figure 5(b) confirms the beneficial effect of decreasing ball diameter on the fineness of the product.

It can be also seen from Fig. 5(b) that finer products can be obtained at higher ball charge ratios. This can be related with the reduction in grinding efficiency as the ball charge ratio declines. In stirred media mill applications, higher ball charge ratios (typically up to 85%) than the conventional grinding systems (40%−50%) were employed [37,39]. The findings in the current study (Figs. 5(b) and (c)) also confirmed that using high ball charge ratios is necessary to achieve finer particle sizes. However, it should be noted that increasing ball charge ratio will cause an increase in power draw of the mill [8,37].

Simultaneous effect of ball charge ratio and stirring speed on particle size is shown in Fig. 5(c). The large magnitude of effect of stirring speed was observed at all the ball charge ratios tested. The contribution of ball charge ratio was apparent particularly at low stirring speeds.

Figure 6 presents the effects of stirring speed, ball diameter and ball charge ratio on energy consumption over 15 min grinding period. Energy consumption was determined to increase by 40−183 kW·h/t with increasing stirring speed, ball diameter and ball charge ratio.

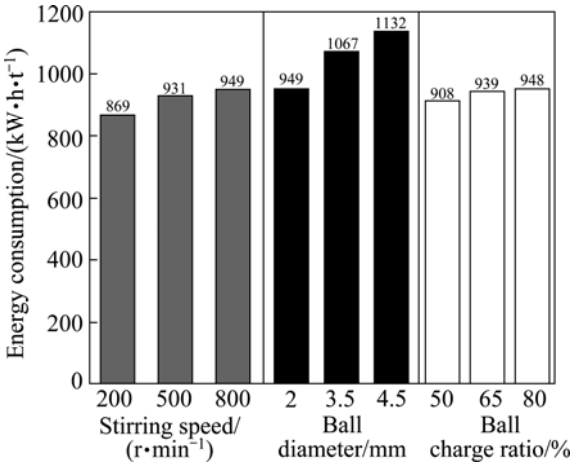


**Fig. 6** Relationship of energy consumption depending on stirring speed (2 mm ball diameter, 65% ball charge ratio), ball diameter (800 r/min stirring speed, 80% ball charge ratio) and ball charge ratio (2 mm ball diameter, 500 r/min stirring speed) with 15 min grinding time

### 3.4 Evaluation of grinding efficiency using stress number and intensity analysis

Figure 7 illustrates the product particle size ($d_{80}$) as a function of stress number at a ball charge ratio of 80%. Particle size had a tendency to decrease with the increase in stress number (Fig. 7). Smaller balls (2 mm) allowed the production of higher stress number and, hence, finer material. KWADE and SCHWEDES [33] reported similar findings for the comminution of limestone in a stirred media mill. However, they also observed no decrease in the product fineness below a critical ball diameter (≤399 μm). These researchers claimed that this adverse effect is due to the fact that in the initial stages of

grinding, small balls cannot generate sufficient stress intensity.

Figure 8 demonstrates the effect of centrifugal stress intensity on product particle size ($d_{80}$) and corresponding stress number at energy consumption levels of 260 and 920 kW·h/t. The optimal stress intensity was identified within the range of $(0.8-2)\times10^{-3}$ N·m while finer material was produced at a high energy consumption, 920 kW·h/t. Outside of this optimal range of stress intensity, coarser material was obtained even at high stress intensities ($>2\times10^{-3}$ N·m). Figure 8 also shows that in the optimal range of stress intensity ($(0.8-2)\times10^{-3}$ N·m), the stress number was also maximized. A similar trend was also observed for gravitational stress intensity (data not shown). This also confirmed that media height (i.e. ball charge ratio) is of practical importance for grinding efficiency. These findings confirmed that stress intensity analysis can be suitably used to determine the optimum conditions of grinding parameters to achieve the desired product fineness.

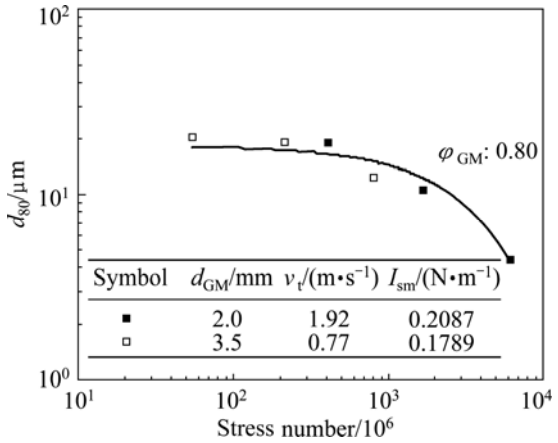


**Fig. 7** Dependency of product particle size ($d_{80}$) on stress number (80% ball charge ratio)

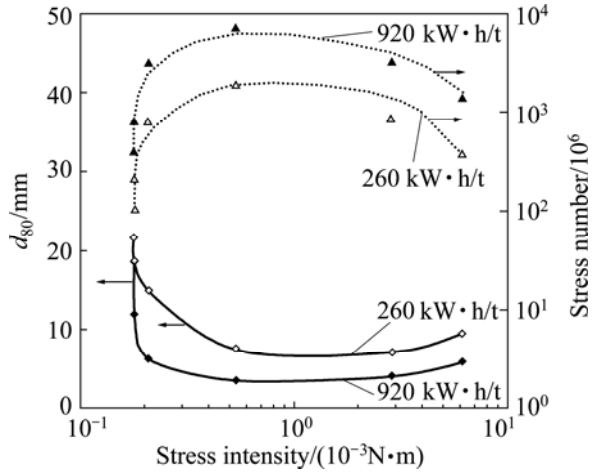


**Fig. 8** Dependency of product particle size and stress number on stress intensity at energy consumptions of 260 and 920 kW·h/t

## 4 Conclusions

Application of ultra fine grinding to cyanidation plant tailings as a potential treatment method for the recovery of silver contained was studied. The effects of ball diameter (2−4.5 mm), stirring speed (200−800 r/min) and ball charge ratio (50%−80%) on ultra-fine grinding of the tailings were demonstrated at three levels using a Box−Behnken design. The findings showed that stirring speed, media size and ball charge ratio were statistically significant parameters regarding their contributions to the fineness of the product. A regression model with a coefficient of determination ($R^2$) of 0.96 was derived. It was shown that a product finer than 5 μm can be produced under the suitable conditions using ceramic beads. The finest product with $d_{80}$ of 2.73 μm was obtained under the conditions of ball diameter of 2 mm, stirring speed of 800 r/min and ball charge ratio of 80% over 15 min. Energy consumption was increased with increasing the level of each grinding parameter tested. The grinding process was controlled closely by the stress intensity, which had an optimal range of $(0.8-2)\times10^{-3}$ N·m to obtain a finer product.

## Acknowledgements

The authors would like to express their sincere thanks and appreciation to Dr. İbrahim Alp and Yildizlar Holding for kindly providing the tailings sample, to Dr. Haci Deveci for proof reading the article and to Dakot Milling Media (Pty) Ltd (South Africa) for kindly providing the ceramic micro-grinding beads (DMM AZ 2000®).

## References

[1] la BROOY S R, LINGE H G, WALKER G S. Review of gold extraction from ores [J]. Minerals Engineering, 1994, 7(10): 1213−1241.

[2] DUNN J G, CHAMBERLAIN A C. The recovery of gold from refractory arsenopyrite concentrates by pyrolysis-oxidation [J]. Minerals Engineering, 1997, 10(9): 919−928.

[3] GUNYANGA F P, MAHLANGU T, ROMAN R J, MUNGOSHI J, MBEVE K. An acidic pressure oxidation pre-treatment of refractory gold concentrates from the Kwekwe Roasting Plant-Zimbabwe[J]. Minerals Engineering, 1999, 12(8): 863−875.

[4] IGLESIAS N, CARRANZA F. Refractory gold-bearing ore: A review of treatment methods and recent advances in biotechnological techniques [J]. Hydrometallurgy, 1994, 34: 383−395.

[5] CIFTCI H, AKCIL A. Effect of biooxidation conditions on cyanide consumption and gold recovery from a refractory gold concentrate [J]. Hydrometallurgy, 2010, 104: 142−149.

[6] CORRANS I J, ANGOVE J E. Ultra fine milling for the recovery of refractory gold [J]. Minerals Engineering, 1991, 4(11): 763−776.

[7] MARSDEN J O, HOUSE C L. The chemistry of gold extraction [M]. USA: Society for Mining Metallurgy and Exploration, 2006.

[8] CELEP O, ASLAN N, ALP İ, TAŞDEMIR G. Optimization of some parameters of stirred mill for ultra–fine grinding of refractory Au/Ag ores [J]. Powder Technology, 2011, 208: 121−127.

[9] JANKOVIC A, VALERY W. Fine and ultra fine grinding–the facts and myths [C]//The 6th Annual I.I.R. Crushing and Grinding Conference. Perth: Metso, 2004.
[10] SEPULVEDA J L. A detailed study on stirred ball mill grinding [D]. USA, Salt Lake City: University of Utah, 1981: 278.
[11] JANKOVIC A. Variables affecting the fine grinding of minerals using stirred mills [J]. Minerals Engineering, 2003, 6: 337−345.
[12] CELEP O, ALP İ, TÜRK T. Stirred media mills in ultrafine grinding technology and the applications in ore dressing [J]. Review of Earth Sciences–İstanbul, 2008, 21(2): 61−73.
[13] ORUMWENSE O A, FORSSBERG E. Superfine and ultrafine grinding—A literature survey [J]. Mineral Processing and Extractive Metall Rev, 1992, 11: 107−127.
[14] KWADE A. Wet comminution in stirred media mills–research and its practical application [J]. Powder Technology, 1999, 105: 14−20.
[15] ZHENG J. Stirred media mills: Dynamics, performance and physico–chemical aspects [D]. Colombia, USA: Colombia University, 1997: 119.
[16] KAPUR P C, HEALY T W, SCALES P J, BOGER D V, WILSON D. Role of dispersants in kinetics and energetics of stirred ball mill grinding [J]. International Journal of Mineral Processing, 1996, 47: 141−152.
[17] LICHTER J, DAVEY G. Selection and sizing of ultrafine and stirred grinding mills [M]//Advances in Comminution. Colorado: Society for Mining, Metallurgy and Exploration, 2006.
[18] GAO M W, FORSSBERG E. A study on the effect of parameters in stirred ball milling [J]. International Journal of Mineral Processing, 1993, 37: 45−59.
[19] TÜZÜN M A, LOVEDAY B K, HINDE A L. Effect of pin tip velocity, ball density and ball size on grinding kinetics in a stirred ball mill [J]. International Journal of Mineral Processing, 1995, 43: 179−191.
[20] BOX G E P, HUNTER W G, HUNTER J S. Statistics for experimenters: An introduction to design, data analysis, and model building [M]. New York: Wiley, 1978.
[21] MONTGOMERY D C. Design and analysis of experiments [M]. New York: John Wiley & Sons, 2001.
[22] MYERS R H, MONTGOMERY D C. Response surface methodology: Process and product optimization using designed experiments [M]. New York: Wiley, 2002.
[23] ASLAN N. Application of response surface methodology and central composite rotatable design for modelling and optimization of a multi–gravity separator for chromite concentration [J]. Powder Technology, 2008, 185: 80−86.
[24] ASLAN N, CEBECI Y. Application of Box–Behnken design and response surface methodology for modelling of some Turkish coals [J]. Fuel, 2007, 86: 90−97.
[25] DAVEY G. Ultrafine grinding applications using Metso stirred mills in precious metal processing [C]//The XII International Mineral Processing Symposium. Turkey: Chamber of Mining Engineers of Turkey, 2010.
[26] CELEP O, ALP İ, DEVECI H. Improvement of cyanidation of antimonial refractory gold/silver ores by ultrafine grinding in a stirred mill [C]//The XII International Mineral Processing Symposium. Turkey, 2010.
[27] DINÇER H. Benefication of gümüşköy silver plant tailings and increasing the plant recovery [D] Turkey: İTÜ, 1997: 91.
[28] CELEP O, ALP İ, DEVECI H, VICIL M. Characterization of refractory behaviour of a complex gold/silver ore by diagnostic leaching [J]. Transactions of Nonferrous Metals Society of China, 2009, 19: 707−713.
[29] KOTZE H. Selecting ceramic grinding media [J]. Chemical Engineering Technology, 2012, 35(11): 2051−2057.
[30] MATHEWS P G. Design of experiments with Minitab [M]. Milwaukee: ASQ Quality Press, 2005.
[31] MINITAB. Statistical Software, Minitab Inc., Evaluation version 14.12.0, USA, 2004.
[32] DESIGN–EXPERT. Software for experimental design [M]. USA: Version 7.14 (trial), Stat–Ease Inc., Minneapolis, (2007).
[33] KWADE A, SCHWEDES J. Breaking characteristics of different materials and their effects on stress intensity and stress number in stirred media mills [J]. Powder Technology, 2002, 122: 109−121.
[34] JANKOVIC A. Media stress intensity analysis for vertical stirred mills [J]. Minerals Engineering, 2001, 14(10): 1177−1186.
[35] KWADE A, BLECHER L, SCHWEDES J. Motion and stress intensity of grinding beads in a stirred media mill. Part 2: Stress intensity and its effect on comminution [J]. Powder Technology, 1996, 86: 69−76.
[36] MANKOSA M J, ADEL G T, YOON R H. Effect of operating parameters in stirred ball mill grinding of coal [J]. Powder Technology, 1989, 59: 255−260.
[37] GAO M, HOLMES R. Developments in fine and ultrafine grinding technologies for the minerals industry [EB/OL]. http://www.iom3.org, 2007.
[38] MANKOSA M J, ADEL G T, YOON R H. Effect of media size in stirred ball mill grinding of coal [J]. Powder Technology, 1986, 49: 75−82.
[39] DAVEY G. Fine grinding applications using Metso vertimill grinding mill and the Metso Stirred media detritor (SMD) in gold processing [C]//38th Annual Meeting of the Canadian Mineral Processors. Ottawa, Canada, 2006.

# 立式搅拌细磨难处理银厂尾矿

O. CELEP, E. Y. YAZICI

UFG Group, Division of Mineral & Coal Processing, Department of Mining Engineering,
Karadeniz Technical University, Trabzon 61080, Turkiye

**摘　要**：采用实验室型立式搅拌磨机将银厂尾矿进行超细磨碎。试验证明，将尾矿超细磨碎能大幅度提高尾矿氰化浸出银的提取率，从细磨前尾矿($d_{80}$为 100 μm)中银的浸出率 36%提高到细磨后($d_{80}$为 1.2 μm)的 84%。在超细磨试验中，通过 Box–Behnken 设计，研究了磨球直径(2~4.5 mm)、搅拌速度(200~800 min/min)和球料比(50%~80%)对研磨细度的影响。结果表明，提高搅拌速度和球料比降低了磨料细度，使用较大的磨球会得到较粗大的产品。在适当的条件下，可以得到细度小于 5 μm 的磨料。应力强度分析表明，应力强度范围(0.8~2)×$10^{-3}$ N·m 是合适的。

**关键词**：难处理尾矿；搅拌磨；超细磨；实验设计；Box–Behnken 设计；应力强度

**(Edited by Xiang-qun LI)**